行政院國家科學委員會補助專題研究計畫成果報告

※※※※※※※※※※※※※※※※※※※※※※※※※
※　　　　　　　　　　　　　　　　　　　　　　　※
※　　受振動干擾下之力平衡式速率陀螺儀　　※
※　　　　的非線性動力分析與混沌控制　　　　※
※　　　　　　　　　　　　　　　　　　　　　　　※
※　　　　　　　　　　　　　　　　　　　　　　　※
※※※※※※※※※※※※※※※※※※※※※※※※※

計畫類別：□個別型計畫　　□整合型計畫

計畫編號：NSC　90－2213－E－164－001－

執行期間：90 年 08 月 01 日至 91 年 07 月 31 日

計畫主持人：陳恒輝 助理教授

本成果報告包括以下應繳交之附件：

□赴國外出差或研習心得報告一份

□赴大陸地區出差或研習心得報告一份

□出席國際學術會議心得報告及發表之論文各一份

□國際合作研究計畫國外研究報告書一份

執行單位：修平技術學院機械工程系

中　華　民　國 九十一 年 九 月 二十 日

受振動干擾下之力平衡式速率陀螺儀的非線性動力分析與混沌控制

CONTROLLING CHAOS AND NONLINEAR DYNAMIC ANALYSIS OF A RATE GYRO WITH TORQUE CONTROL IN VIBRATORY SITUATION

計畫編號：NSC 90-2213-E-164-001
執行期限：90 年 08 月 01 日至 91 年 07 月 31 日
主持人：陳恒輝 助理教授 修平技術學院機械工程系
計畫參與人員：江俊顯 講師，蘇詩凱 大專生研究助理 機械系

一、中文摘要

本論文將對一受振動干擾下之力平衡式速率陀螺儀作詳細非線性動力分析與混沌控制析，此時飛行器相對於自轉軸作$\mu_Z(t)$轉動。當飛行器相對於自轉軸作穩態轉動時，利用 Routh-Hurwits 理論對此自治系統作穩定性分析，給出系統參數穩定條件。當飛行器相對於自轉軸作簡諧轉動時，這系統為參數激勵強非線性耗散系統，隨著系統參數變動下，系統呈現規則與混沌反應行為。經由相軌跡、龐加萊截面、平均功率普與李雅普若夫指數等數值模擬方法來分析系統，發現隨系統參數變化，系統存在數種不同型態的解與分歧行為如 Hopf 分歧、對稱分歧與倍週期分歧，並得到系統混沌行為。並在適當的力矩回饋控制下能有效地抑制混沌運動。

關鍵詞：速率陀螺儀、分歧、混沌

Abstract

An analysis of stability and chaotic dynamics is presented of a single-axis rate gyro with torque control in vibratory situation. For the autonomous case in which the vehicle undergoes a steady rotation, the necessary and sufficient conditions for stability of the system were provided by Routh-Hurwitz theory. Also, the degeneracy conditions of the nonhyperbolic point were derived. The stability of the nonlinear nonautonomous system was investigated by Liapunov stability and instability theorems. As the electrical time constant is much smaller than the mechanical time constant, the singularly perturbed system was obtained by the singular perturbation theory. The Liapunov stability of this system by studying the reduced and boundary-layer systems was also analyzed. The numerical simulations were performed to verify the analytical results. The stability regions of the autonomous system were obtained in parametric diagrams. For the nonautonomous case in which $\mu_Z(t)$ oscillates near stability boundary, periodic, quasiperiodic and chaotic motions were demonstrated by using time history, phase plane and Poincaré maps.

Keywords: Rate Gyro, Bifurcation, Chaos

二、Introduction

The field of application of gyroscopes is widespread, such as in the navigation and control system, owing to its distinctive property. Here, a single-axis rate gyro is used for the measurement of angular velocity in spinning space vehicles. For all applications, it is a critical problem to show the stability of motion of the gyro, both theoretically and practically.

Several interesting problems have been studied previously in the analysis of motion of the gimbal of rate gyros in spinning vehicles [1-4]. For the case in which $_Z$ is uncertain and constant, using the Liapunov approach, conditions for global and local asymptotic stability of the gyro in spinning vehicles have been obtained [1]. The motion of a single-axis rate gyro in consideration of the angular velocity of vehicle about its spin axis and the angular acceleration of the vehicle about its output axis has been examined for small rotation of the gimbal [2-3]. The stability of a rate gyro mounted on a vehicle, which has a time-varying angular velocity about its spin of the gyro, is studied by the Liapunov direct method [4]. All of them are two-dimensional systems. An analysis of stability and chaotic dynamics is presented of a rate gyro with feedback control mounted on a space vehicle that is spinning with uncertain angular velocity $_Z(t)$ about its spin of the gyro [5]. This system is a three-dimensional nonlinear one.

A nonlinear system can also exhibit complicated steady state behaviors referred as to chaos in some parametric space [6]. The chaotic attractor so called “deterministic chaos” that was discovered by Lorenz in the numerical study of meteorology. Chaotic motions whose time histories have a sensitive dependence on initial

conditions occur when some nonlinearities exist [6-10]. There are many routes to chaos in dissipative systems. Three prominent routes to chaos have been explored, including period doubling, intermittency, and Quasiperiodic routes, and related to period doubling, saddle node, and Hopf bifurcations respectively [6-8]. In gyroscopic systems, the dynamics of gyros also exhibit chaotic behavior. In this paper, the parametrically excited system is studied and exhibits the nonlinear phenomena including the existence of periodic, quasiperiodic and chaotic motions of the system.

Singular perturbations, traditional efficient tools for determining physically meaningful subsystems, are developing into systematic approach to multi-time dynamic systems. These methods applied in power systems and Markov chains are used to decompose the dynamic systems into reduced (slow) and boundary-layer (fast) systems [11-12]. The singular perturbation method is also used to derived the special form of the gyro system.

In this paper, the stability and chaotic dynamics of a single-axis rate gyro with torque control in vibratory situation are studied. The controller of the system is modeled by the first order dynamic with a time constant of $O(1)$ so that the feedback control system is a three-dimensional one. For the case in which μ_Z is uncertain and constant, the stability conditions and bifurcation surfaces of the system were derived by Routh-Hurwitz theory and local bifurcation analysis. For the nonlinear nonautonomous system, the stability of the feedback control system will be obtained by using the Liapunov direct method. When the time constant of controller is much smaller than the mechanical time one, the singularly perturbed system is obtained by singular perturbation theory. The Liapunov stability of this system is also analyzed by studying the reduced and boundary-layer systems. Finally, the degeneracy conditions of the system are presented in parametric planes by numerical simulation. The numerical results of the perturbation of an uncertain angular velocity undergoing small harmonic excitation are carried out to examine the various forms of dynamic behavior by using the time history, phase plane, Poincaré maps.

三、Equations of Motion

We consider the model of a single-rate gyro mounted on a space vehicle as shown in figure 1. The gimbal can turn about output X axis with rotational angle θ. Motion about this axis is resisted by damping torque defined by $f_d(\dot{\theta})$. Using Largrange's equation, the differential equation for the output deflection angle θ of a rate gyro with feedback control was derived as follows[13]:

$$(A+A_g)\ddot{\theta}+f_d(\dot{\theta})+Cn_R(\mu_Y\cos\theta+\mu_Z\sin\theta)+(A+B_g-C_g)(\mu_Y\cos\theta+\mu_Z\sin\theta)(\mu_Y\sin\theta-\mu_Z\cos\theta)+(A+A_g)\dot{\mu}_X=T_c, \quad (1)$$

where

$$Cn_R = C(\dot{\Omega}-\mu_Y\sin\theta+\mu_Z\cos\theta)=const.,$$

$f_d(\dot{\theta}) = l_1\dot{\theta}+l_3\dot{\theta}^3+\ldots+l_r\dot{\theta}^r$, r : odd number, $l_1>0$, and $f_d(\dot{\theta})\dot{\theta}>0$.

μ_X, μ_Y, and μ_Z denote the angular velocity components of the platform along output axis X, input axis Y, and normal axis Z, respectively. A, A (=B), C and A_g, B_g, C_g denote the moments of inertia of rotor and gimbal, respectively, about the gimbal axes ¶, ¡, ¸. T_c is the control-motor torque along the output axis of the system to balance the corresponding gyroscopic torque. The torque and electric current of control-motor can be modeled by the following relationship:

$$T_c = K_T I, \quad (2)$$

$$L\dot{I}+RI = K_a(\theta_d-\theta)-K_0\dot{\theta}, \quad (3)$$

where electromotive force proportional to the difference between the prescribed motion $\theta_d(t)$ and the rotational angle θ, that is $u=K_a(\theta_d-\theta)$, is applied to the control-motor. I, R, L, and K_0 are the current, resistance, inductance, and back-electromotive constant of the control-motor; K_T denotes the torque constant of the control-motor.

Equations (1)-(3) thus represent a feedback control system in which position feedback is applied to the gyro motion. The prescribed motion of the gyro is desired to be fixed at the origin, i.e. $\theta_d=0$, in which the relationship of the output angle θ proportional to the input angular velocity μ_Y is held. Thus, it is very important to analyze the stability of the measuring origin of a rate gyro system mounted in a wobbling space vehicle, because the more precise analysis for the system, the more reliability for the guidance.

We are interested in the nonlinear behavior of dynamical motion when the vehicle undergoes uncertain angular velocity $\mu_Z(t)$ about the spin axis (Z-axis), acceleration $\dot{\mu}_X(t)$ about the output axis (X-axis), and the angular velocity about OY is zero, i.e., $\mu_Y=0$. Now the feedback control system is studied in the following form

$$\dot{x}=y,$$

$$\dot{y}=-D_1(y)+D_2z-D_3\mu_Z(t)\sin x+1/2D_4\mu_Z^2(t)\sin 2x-\dot{\mu}_X,$$

$$\dot{z}=-D_5z-D_6x-D_7y, \quad (4)$$

where

$$x=\theta, y=\dot{\theta}, z=I, \quad D_1(\dot{\theta})=f_d(\dot{\theta})/(A+A_g),$$

$$D_2=K_T/(A+A_g),\ D_3=Cn_R/(A+A_g),$$

$$D_4=(A+B_g-C_g)/(A+A_g), \quad D_5=R/L,$$

$$D_6=K_a/L,\ D_7=K_0/L.$$

In this section, the stability of both autonomous system and nonautonomous system are discussed by

distinct methods. The stability of the autonomous system is analyzed to obtain the necessary and sufficient conditions for locally asymptotical stable motion at the fixed point by Routh-Hurwitz criterion. In addition, the Liapunov direct method [13] is used to obtain the conditions sufficient for asymptotical stability and instability of motion of the feedback control system.

3.1 The stability of the nonlinear autonomous system

For the case when $\dot{\mu}_X = 0$ and $\mu_Z=\mu_{ZC}=const.$, this system is autonomous. One stationary point of the nonlinear autonomous system is the origin $(x, y, z)=(0, 0, 0)$. Let the disturbed motion as $x=0+x_1$, $y=0+x_2$, $z=0+x_3$, the equations for disturbances are as:

$$\dot{x}_1 = x_2,$$
$$\dot{x}_2 = -D_{11}x_2 + D_2x_3 - D_3\mu_{ZC}x_1 + D_4\mu_{ZC}^2x_1 - h(\mu_{ZC})x_1^3 - D_{12}x_2^3 + O(x_1, x_2)^5,$$
$$\dot{x}_3 = -D_5x_3 - D_6x_1 - D_7x_2, \quad (5)$$

where $D_{11}=l_1/(A+A_g)$, $D_{12}= l_3/(A+A_g)$, $h(\mu_{ZC})= -D_3\mu_{ZC}/6+2D_4\mu_{ZC}^2/3$.

The stability analysis of the origin of the autonomous system will be studied by the Routh-Hurwitz criterion as follows.

First, we obtain the Jacobian matrix $\boldsymbol{J}$ at the origin of the system (5) in the form of

$$\boldsymbol{J}=\begin{bmatrix} 0 & 1 & 0 \\ Q & -D_{11} & D_2 \\ -D_6 & -D_7 & -D_5 \end{bmatrix}, Q= -D_3\mu_{ZC}+D_4\mu_{ZC}^2, \quad (6)$$

and the characteristic equation of $\boldsymbol{J}$ in the form of

$$\lambda^3+(D_5+D_{11})\lambda^2+(D_2D_7-Q+D_{11}D_5)\lambda -QD_5 +D_6D_2=0 \text{ or } \lambda^3+a_1\lambda^2+a_2\lambda+a_3=0. \quad (7)$$

The Hurwitz matrix $\boldsymbol{H}$ for the above polynomial is

$$\boldsymbol{H}=\begin{bmatrix} a_1 & 1 & 0 \\ a_3 & a_2 & a_1 \\ 0 & 0 & a_3 \end{bmatrix}. \quad (8)$$

The necessary and sufficient conditions for all the roots of characteristic equation (7) to have negative real parts are provided by the Routh-Hurwitz criterion, i.e., the principle minors of the Hurwitz matrix $\boldsymbol{H}$ must all be positive. So, the stability conditions are obtained as follows

$$D_5+ D_{11}>0, \quad (9.a)$$
$$D_5D_2D_7+D_{11}D_5^2+D_{11}D_2D_7-D_{11}Q+D_{11}^2D_5-D_6D_2>0, \text{ i.e., } e_1\mu_{ZC}^2+e_2\mu_{ZC}+e_3>0, \quad (9.b)$$
$$-QD_5+D_6D_2>0, \text{ i.e., } e_4\mu_{ZC}^2+e_5\mu_{ZC}+e_6>0, \quad (9.c)$$

where $e_1=e_4=-D_4<0$, $e_2=e_5=D_3$, $e_6=D_6D_2/D_5$, $e_3=(D_5D_2D_7+D_{11}D_5^2+D_{11}D_2D_7+D_{11}^2D_5-D_6D_2)/D_{11}$

The above stability conditions can be rewritten as

$$\mu_{ZC1} < \mu_{ZC} < \mu_{ZC2}, \quad (10.a)$$

where

$$\mu_{ZC1}=[-e_2-(e_2^2-4e_1p_{\min})^{1/2}]/(2e_1)=[D_3-(D_3^2-4D_4p_{\min})^{1/2}]/(2D_4), \quad (10.b)$$
$$\mu_{ZC2}=[D_3+(D_3^2-4D_4p_{\min})^{1/2}]/(2D_4), p_{\min}=Min(e_3,e_6). \quad (10.c)$$

That all the roots of the characteristic polynomial (7) of the Jacobian matrix $\boldsymbol{J}$ have negative real parts, i.e., the motion of the linearized autonomous system is asymptotically stable at the fixed point. Alternatively, the system possesses critical behavior when Jacobian matrix $\boldsymbol{J}$ contains the eigenvalues with zero real parts in the following bifurcation surfaces:

1. There exists one zero eigenvalue ($\lambda_1=0$) of this linearized system for the system parameter $Q=D_6D_2/D_5$, i.e., $\mu_{ZC}=\mu_{ZC1}$ or μ_{ZC2}, on stability boundary, $p_{\min}=e_6$. The residual eigenvalues are $\lambda_{2,3}=\{-(D_{11}+D_5)\pm[(D_{11}+D_5)^2-4(D_2D_7-Q+D_{11}D_5)]^{1/2}\}/2$;
2. There exists a pair of pure imaginary eigenvalues ($\lambda_{1,2}=\pm j\mu_0$) of this linearized system for the system parameter $Q=(D_5D_2D_7+D_{11}D_5^2+D_{11}D_2D_7+D_{11}^2D_5-D_6D_2)/D_{11}$, i.e., $\mu_{ZC}=\mu_{ZC1}$ or $\mu_{ZC}=\mu_{ZC2}$, $p_{\min}=e_3$., where $\mu_0=(-D_{11}(D_5D_2D_7+D_{11}D_5^2-D_6D_2))^{1/2}/D_{11}$ is a real number, i.e., $D_2>D_{11}D_5^2/(D_6 -D_5D_7)$. The residual eigenvalue is $-(D_{11}+D_5)$;
3. There exists a double zero eigenvalues ($\lambda_{1,2}=0,0$) for (a) the system parameter $Q=D_{11}D_5D_6/(D_6 -D_5D_7)$ and $D_2=D_{11}D_5^2/(D_6 -D_5D_7)$, the residual eigenvalue is $-(D_{11}+D_5)$; (b) the system parameter $Q=D_6D_2/D_5$ and $D_{11}=D_2(D_6 -D_5D_7)/ D_5^2$, the residual eigenvalue is still in the form of $-(D_{11}+D_5)$ but the value adapts for varying the system parameter D_{11},

where $Q=-D_3\mu_{ZC}+D_4\mu_{ZC}^2$, $D_{11}=l_1/(A+A_g)$, $D_2=K_7/(A+A_g)$.

3.2 The stability of the nonautonomous system

For the case when $\dot{\mu}_X(t)$ and $\mu_Z(t)$ are time-varying function, the syetem is the nonautonomous system and the motion of the system (4) can be solved analytically, approximately or numerically as $x=\bar{}_0(t), y=\dot{\bar{}}_0(t), z=I_0(t)$, which satisfies the following equation:

$$\ddot{\bar{}}_0+D_1(\dot{\bar{}}_0)+D_3\mu_Z\sin\bar{}_0-1/2D_4\mu_Z^2\sin2\bar{}_0+\dot{\mu}_X=D_2I_0, \quad (11.a)$$
$$\dot{I}_0+D_5I_0 = -D_6\bar{}_0-D_7\dot{\bar{}}_0. \quad (11.b)$$

Let the disturbed motion be $x=\bar{}_0(t)+x_1, y=\dot{\bar{}}_0(t)+x_2, z=I_0(t)+x_3$, where x_1, x_2, x_3 are deviations from their respective nominal conditions. The differential equation (4) for the disturbances is

$$\dot{x}_1 = x_2,$$
$$\dot{x}_2 = -D_{11}x_2 + D_2x_3 - D_3\mu_Z(t)x_1 + D_4\mu_Z^2(t)x_1 - h_0(\mu_Z(t))x_1^2 - D_{12}x_2^3 - h(\mu_Z(t))x_1^3 + O(x_1,x_2)^4$$
$$\dot{x}_3 = -D_5x_3 - D_6x_1 - D_7x_2, \quad (12)$$

where $D_{3t}=D_3\cos(\bar{}_0(t)), D_{4t}=D_4\cos(2\bar{}_0(t))$, $h_0(\mu_Z(t))=D_{3t}\mu_Z(t)/2-D_{4t}\mu_Z^2(t), h(\mu_Z(t))= -D_{3t}\mu_Z(t)/6+2D_{4t}\mu_Z^2(t)/3$.

The stability of the motion of the above system (12) is investigated by the Liapunov direct method. Now we take the Liapunov function of quadratic forms:

$$V(a_1, a_2)= a_1x_1^2/2+ a_2x_1x_2+x_2^2/2+ a_2D_2x_3^2/(2D_6), \quad (13)$$

where a_1 and a_2 are undertermined positive constants. There exists a number of Liapunov function candidates varied with the proper value of a_1, a_2, in which each of Liapunov candidates can give the conditions sufficient for stability. By choosing a number of a_1, a_2 properly, we can obtain the conditions sufficient for asymptotical stability of motion of the feedback control system. We have the negative time derivative of V through equation (12) as

$$-\dot{V}(a_1, a_2) = a_2[D_{3t}\mu_Z(t)-D_{4t}\mu_Z^2(t)]x_1^2+[a_2D_{11}+D_{3t}\mu_Z(t)-a_1-D_{4t}\mu_Z^2(t)]x_1x_2+(D_{11}-a_2)x_2^2+(a_2D_8-D_2)x_2x_3+a_2D_9x_3^2+W_1^* \quad (14)$$

where $D_8=D_2D_7/D_6$, $D_9=D_2D_5/D_6$, and W_1^* represents higher order terms.

Since $-\dot{V}$ contains time explicitly, we must find a function W that does not contain time explicitly such that $-\dot{V} \geq W$. We take W as:

$$W= a_2(D_2+a_3)x_1^2+(a_2D_{11}+D_2-a_1+a_3)x_1x_2+a_2x_2^2+(a_2D_8-D_2)x_2x_3+a_4x_3^2, \quad (15)$$

where a_3 and a_4 are undertermined positive constants. By Sylvester's theorem[13], W is positive definite if

$$a_2 > 0, \quad (16.a)$$

$$a_3 > -D_2 = -K_T/(A+A_g), \quad (16.b)$$

$$(D_{11}a_2+D_2+a_3)-\sqrt{a_2(D_2+a_3)[4a_2a_4-(D_8a_2-D_2)^2]/a_4} < a_1 < (D_{11}a_2+D_2+a_3)+\sqrt{a_2(D_2+a_3)[4a_2a_4-(D_8a_2-D_2)^2]/a_4} \quad (16.c)$$

$$a_4 > (D_2-a_2D_8)^2/(4a_2) > 0, \quad (16.d)$$

are satisfied. Furthermore,

$$-\dot{V}-W= a_2[-D_2+(D_{3t}\mu_Z-a_3)-D_{4t}\mu_Z^2]x_1^2+[-D_2+(D_{3t}\mu_Z-a_3)-D_{4t}\mu_Z^2]x_1x_2+(D_{11}-2a_2)x_2^2+(D_9a_2-a_4)x_3^2+W^* \quad (17)$$

where W^* represents the terms of higher degree. If the following inequalities are held, then $-\dot{V}-W \geq 0$ (= 0 only when $x_1=0, x_2=0, x_3=0$), i.e., $-\dot{V}-W$ is positive definite. So $-\dot{V}$ is positive definite:

$D_{4t} > 0$, i.e., $-\pi/4 < \theta_0 < \pi/4$

$$(D_{3t}-\sqrt{D_{3t}^2-4D_{4t}(D_2+a_3)})/(2D_{4t}) < \mu_Z < (D_{3t}+\sqrt{D_{3t}^2-4D_{4t}(D_2+a_3)})/(2D_{4t}) \quad (18.a)$$

$$a_3 < D_{3t}^2/(4D_{4t}) - D_2 \quad (18.b)$$

$$D_{11} > 2a_2 > 0 \quad (18.c)$$

$$4a_2(D_{11}-2a_2)-[-D_2+(D_{3t}\mu_Z-a_3)-D_{4t}\mu_Z^2] > 0, \text{ i.e.,} \quad (18.d)$$

If $a_3 < D_{3t}^2/4D_{4t} - D_2 - 4a_2(D_{11}-2a_2)$, then

$$\mu_Z < (D_{3t}-\sqrt{D_{3t}^2-4D_{4t}[(D_2+a_3)+4a_2(D_{11}-2a_2)]})/(2D_{4t}) \quad \text{or}$$

$$\mu_Z > (D_{3t}+\sqrt{D_{3t}^2-4D_{4t}[(D_2+a_3)+4a_2(D_{11}-2a_2)]})/(2D_{4t}). \quad (18.e)$$

If $a_3 > D_{3t}^2/(4D_{4t}) - D_2 - 4a_2(D_{11}-2a_2)$, then

$$\mu_Z \in \Re \quad \Re: real\ number. \quad (18.f)$$

$$a_4 < D_9a_2 \quad (18.g)$$

By Sylvester's theorem, the sufficient condition for the positive definiteness of V is

$$a_1 > a_2^2 > 0. \quad (19)$$

From equations (16.c), (16.d) and (19), we have

$a_L < a_1 < a_H$, where

$$a_L=(a_2, D_{11}a_2+D_2+a_3-\sqrt{a_2(D_2+a_3)[4a_2a_4-(D_8a_2-D_2)^2]/a_4})_{ma}, \quad (20.a)$$

$$a_H=D_{11}a_2+D_2+a_3+\sqrt{a_2(D_2+a_3)[4a_2a_4-(D_8a_2-D_2)^2]/a_4}. \quad (20.b)$$

From equations (16.b) and (18.c), we have

$$a_H > 2a_2^2+D_2+a_3+\sqrt{a_2(D_2+a_3)[4a_2a_4-(D_8a_2-D_2)^2]/a_4} > a_2^2. \quad (21)$$

So the parameter a_1 can be chosen in the domain constrained by the above inequalities. Similarly by the former inequalities (16.b), (18.b), (18.e) and (18.f), we know that a_3 can be chosen if

$$-D_2 < a_3 < D_{3t}^2/4D_{4t} - D_2 \quad (22)$$

is held. From equations (16.d) and (18.g), the parameter a_4 also can be chosen as:

$$(D_2-D_8a_2)^2/(4a_2) < a_4 < D_9a_2, \text{ i.e.,} \quad (23)$$

the following inequalities are held

$$a_2 > D_2/D_8 \quad for D_8 < 2\sqrt{D_9}, \quad (24.a)$$

$$a_2 > D_2/(2D_8) \quad for\ D_8 = 2\sqrt{D_9}, \quad (24.b)$$

$$D_2/(2\sqrt{D_9}+D_8) < a_2 < D_2/(D_8-2\sqrt{D_9}) \quad for\ D_8 > \quad (24.c)$$

.

From equations (18.a), (18.c), (18.e), and (18.f) by properly selecting a suitable a_2 of equation (24), and a number of a_3 of equation (22), we can get the following conditions that assure both $V(a_1, a_2)$ and $-\dot{V}(a_1, a_2)$ are positive definite:

$\mu_{Z1}=0 < \mu_Z < \mu_{Z2}=D_{3t}/D_{4t}$, and (25a)

$D_{11} > 2a_2$, (25b)

a_2 can be taken from equation (24).

According to the Liapunov asymptotical theorem, the equation (25) is the condition sufficient for stability of the system, and the motion $(\theta, \dot{\theta}, I)=(\theta_0, \dot{\theta}_0, I_0)$ is asymptotically stable.

The conditions sufficient for instability of motion of the feedback control system are considered by using the Liapunov instability theorem. We construct the Liapunov function as

$$V(m_1, m_2) = -m_1x_1^2/2-m_2x_1x_2+x_2^2/2+m_2D_2x_3^2/(2D_6) \quad (26)$$

where m_1 and m_2 are undetermined positive constants. Then we have

$$-\dot{V}(m_1, m_2) = -m_2[D_{3t}\mu_Z(t)-D_{4t}\mu_Z^2(t)]x_1^2+[-m_2D_{11}+D_{3t}\mu_Z(t)+m_1-D_{4t}\mu_Z^2(t)]x_1x_2+2m_2D_2x_1x_3+(D_{11}+m_2)x_2^2+(m_2D_8-D_2)x_2x_3+m_2D_9x_3^2+W_2^* \quad (27)$$

where W_2^* represents the terms of higher degree.

Since $-\dot{V}$ contains time explicitly, we must find a function W that does not contain time explicitly such that $-\dot{V} \geq W$. We take W as:

$$W= -m_2\dot{e}x_1^2+(\dot{e}-m_2D_{11}+m_1)x_1x_2+m_2x_2^2+2m_2D_2x_1x_3+(m_2D_8-D_2)x_2x_3+m_3x_3^2 \quad (28)$$

where $0 > e^{-} > -\infty$. By Sylvester's theorem, we know that W is positive definite if

$m_L < m_1 < m_H$, where

$$m_L = D_{11} m_2 - e^{-} - 2m_2\sqrt{-e^{-}},$$

$$m_H = D_{11} m_2 - e^{-} + 2m_2\sqrt{-e^{-}} \quad (29.a)$$

$$m_{av} = D_{11} m_2 - e^{-} + D_2 m_2 (D_8 m_2 - D_2)/m_3,$$

$$m_D = \sqrt{m_2 (D_2^2 m_2 + e^{-} m_3)[(D_8 m_2 - D_2)^2 - 4m_2 m_3]/m_3^2}, \quad (29.b)$$

$m_2 > 0$

$0 < m_3 < (D_8 m_2 - D_2)^2/(4m_2)$, for $0 > e^{-} > -m_2 D_2^2/m_3$ (29.d)

$m_3 > (D_8 m_2 - D_2)^2/(4m_2)$, for $e^{-} < -m_2 D_2^2/m_3$ (29.e)

are satisfied. Furthermore,

$$-\dot{V} - W = m_2(e^{-} - D_{3t}\mu_Z + D_{4t}\mu_Z^2)x_1^2 + (-e^{-} - D_{3t}\mu_Z - D_{4t}\mu_Z^2)x_1 x_2 + D_{11} x_2^2 + (m_2 D_9 - m_3)x_3^2. \quad (30)$$

If the following inequalities hold, then $-\dot{V} - W \geq 0$, i.e., $-\dot{V}$ is positive definite:

$D_{4t} > 0$, i.e., $-\pi/4 < \bar{\ }_0 < \pi/4$,

$$\mu_Z < (D_{3t} - \sqrt{D_{3t}^2 - 4D_{4t}e^{-}})/(2D_{4t}) \text{ or } \mu_Z > (D_{3t} + \sqrt{D_{3t}^2 - 4D_{4t}e^{-}})/(2D_{4t}), \quad (31.a)$$

$D_{11} > 0$ (31.b)

$$(D_{3t} - \sqrt{D_{3t}^2 - 4D_{4t}e^{-} + 16D_{11}D_{4t}m_2})/(2D_{4t}) < \mu_Z < (D_{3t} + \sqrt{D_{3t}^2 - 4D_{4t}e^{-} + 16D_{11}D_{4t}m_2})/(2D_{4t}), \quad (31.c)$$

$m_3 < m_2 D_9$. (31.d)

From equations (29.a), and (29.b), if $m_L < m_{av} < m_H$ are satisfied, i.e., $(0, (D_2^2 - 2\sqrt{-e^{-}})/(D_2 D_8))_{\max} < m_2 < (D_2^2 + 2\sqrt{-e^{-}})/(D_2 D_8)$, the parameter m_1 can be chosen. Similarly by the former inequalities (29.d), (29.e) and (31.d), we know that m_3 can be selected. Also from equations (31.a), (31.b), and (31.c), by properly selecting a number of e^{-}, we can get the conditions that assure $-\dot{V}(m_1, m_2)$ are positive definite:

$\mu_Z < 0$ or $\mu_Z > D_{3t}/D_{4t}$ (32.a)

$D_{11} > 0$ (32.b)

According to the Liapunov instability theorem, equations (32.a) and (32.b) are the condition sufficient for the unstable system. From the previous result, we can obtain conditions for sufficient of stability and instability of the motion $(\bar{\ }, \dot{\bar{\ }}, I) = (\bar{\ }_0, \dot{\bar{\ }}_0, I_0)$.

4. SINGULAR PERTURBATION MODEL

To facilitate the analysis, in the interest of model simplification, we usually neglect these small physical parameters to reduce the order of this model. Singular perturbations are used to simplify the model and to provide tools for improving oversimplified models when the original full order model satisfies the some assumptions [11]. To obtain the standard singular perturbation model, let us define the variables

$p_1 = x$, $p_2 = T_m y$, $q = (T_m^2 D_2) z$, $t \to t/T_m$,

$T_m = D_5/(D_{11}D_5 + D_2 D_7)$, $T_e = 1/D_5 = L/R$,

$\varepsilon = T_e / T_m$,

and rewrite the state equation (4) as

$$\dot{p}_1 = p_2,$$

$$\dot{p}_2 = -a_0 p_2 + q - a_3\mu_Z(t)\sin p_1 + 1/2\, a_4\mu_Z^2(t)\sin 2p_1 - \dot{\mu}_X(t),$$

$$\varepsilon\dot{q} = -q - a_1 p_1 - a_2 p_2,$$

or in the compact form $m_L - m_D < m_1 < m_{av} + m_D$, where

$$\dot{p} = f_0(t, p, q, \varepsilon)$$
$$\varepsilon\dot{q} = g_0(t, p, q, \varepsilon) \quad (33)$$

where

$p = [p_1, p_2]$, $f_0 = [f_{01}, f_{02}]$, $a_0 = D_1/T_m$, (29.c)

$a_1 = D_2 D_6 T_m^2 / D_5$, $a_2 = D_2 D_7 T_m / D_5$,

$a_3 = D_3 T_m^2$, $a_4 = D_4 T_m^2$.

We assume that $\varepsilon << 1$. This assumption means that the mechanical time constant T_m is sufficiently larger than the electrical time constant T_e. By using the singular perturbation theory [12] to consider the singularly perturbed system (33), at $\varepsilon = 0$, the slow manifold is

$q = h(t, p) = -a_1 p_1 - a_2 p_2$.

The corresponding slow model, $\dot{p} = f_0(t, p, h(t, p), 0)$,

$$\dot{p}_1 = p_2,$$

$$\dot{p}_2 = -a_1 p_1 - (a_0 + a_2)p_2 - a_3\mu_Z(t)\sin p_1 + 1/2\, a_4\mu_Z^2(t)\sin 2p_1 - \dot{\mu}_X, \quad (34)$$

has an exponentially stable motion $(p_1, \dot{p}_1) = (p_{10}(t), \dot{p}_{10}(t))$ when the following condition is held:

$$\mu_{Z1} < \mu_Z(t) < \mu_{Z2} \quad (35)$$

where

$$\mu_{Z1} = (a_{3t} - \sqrt{a_{3t}^2 + 4a_1 a_{4t}})/(2a_{4t}) = (D_{3t} - \sqrt{D_{3t}^2 + 4D_2 D_{4t}(D_6/D_5)})/(2D_{4t}),$$

$$\mu_{Z2} = (a_{3t} + \sqrt{a_{3t}^2 + 4a_1 a_{4t}})/(2a_{4t}) = (D_{3t} + \sqrt{D_{3t}^2 + 4D_2 D_{4t}(D_6/D_5)})/(2D_{4t})$$

and $D_{4t} > 0$, i.e., $-\pi/4 < \bar{\ }_0 < \pi/4$, $D_{3t} = D_3\cos(\bar{\ }_0)$, $D_{4t} = D_4\cos(2\bar{\ }_0)$.

which can be derived by the same form of Liapunov functions as reference [4]. The origin of the corresponding boundary-layer system

$$\frac{d\psi}{d\tau} = g_0(t, p, \psi + h(t, p), 0) = -\psi$$

is exponentially stable uniformly in (t, p). Since f_0 and g_0 of equation (33) also satisfy the conditions of Appendix (I), we conclude that the origin of the full singularly perturbed system (33) is exponentially stable for sufficiently small ε. Thus, the necessary and sufficient condition for asymptotic stability is the equation (35).

From Sections 3 and 4 analyses, the condition (25) sufficient for asymptotical stability of Section 3 are covered by that (35) of Section 4, i.e.,

$$\mu_{Z1} < \left\{ \begin{matrix} 0 < \mu_Z(t) < D_{3t}/D_{4t} & Eq.(25) \\ \mu_Z(t) & Eq.(35) \end{matrix} \right\} < \mu_{Z2},$$

The result of Section 4 has larger stability region than that of Section 3. In Section 3, a three-dimensional dynamic system is considered. In Section 4, we consider the case in which the mechanical time constant

is sufficiently larger than the electrical time constant. Thus the system can be reduced to a two-dimensional system by singular perturbations which simply the order of the model and provide tools for improving oversimplified models.

四、Numerical Simulations and Discussion

In this section, examples are carried out to examine the various forms of dynamic behavior of the system (4) for the previous analyses by numerical simulation techniques. The parameters of the cases are shown in the Appendix (II).

In section 3.1, the stability condition (10) for the nonlinear autonomous system is derived and the numerical simulations of the autonomous system (5) near the double-zero degenerate point are analyzed. The double-zero eigenvalues with the third eigenvalue a_3= –165 of the system and the stability boundary of the uncertain constant angular velocity μ_{ZC} are obtained corresponding the double-zero degenerate point (D_2, Q) = (388.889,3888.89) or (D_1, Q) = (140,3888.89) depicted in figure 2 and 8. There exists at least one zero eigenvalue of the system at $Q=e_6$, the maximum eigenvalue that is equal to zero is presented by the solid line and the stability boundary of the uncertain constant angular velocity μ_{ZC} corresponding $Q=e_6$ are obtained as shown in figure 3 and 9. A pair of pure imaginary eigenvalues exist corresponding the solid line of $Q=e_3$ and the stability boundary of the uncertain constant angular velocity μ_{ZC} corresponding $Q=e_3$ are obtained in figure 4 and 10. Stability regions of the autonomous system (5) near the double-zero degenerate point are obtained as shown in figure 5 and 11 when both the inequalities conditions $Q < e_6$ and $Q < e_3$ are satisfied. The time history trajectories of the perturbed motion that converge to the origin from the initial state (x_1, x_2, x_3)=(0.1,0,0) are plotted in figures 6(b)-(c) for 'b' and 'c' points within stability region in figure 5. These systems are local asymptotical stable. On the other hand, figures 6(a) and (d) show that the trajectories move far away from the origin to another fixed point and limit cycle, respectively, for 'a' and 'd' points beyond stability region in figure 5. This means that the systems are unstable. Similarly, the phase trajectories corresponding figure 6 are present as shown in figure 7. In figures 12–13, the time histories and phase trajectories for stability and instability also are observed for D_1-Q parameter plane in figure 11.

From stability analyses of the nonautonomous system, in Section 3.2 and 4, the sufficient condition (25) for stability are covered by condition (35) and the latter must satisfy the condition in which the mechanical time constant is sufficiently larger than the electrical time constant. Then those are very close. When the parameters of the gyro satisfy the stability condition, i.e., $\mu_{Z1} < \mu_Z < \mu_{Z2}$, the motion is asymptotically stable.

For the case $\dot{\mu}_X(t)$ is time-varying function but small, the solution of the dynamic system can be assumed zero. In the parameters D_1=1, D_2=10, we have the limits μ_{Z1} = 0, μ_{Z2} = 2000 for the stability condition (25), and the limits μ_{Z1} = -0.05, μ_{Z2} = 2000.05 for the stability condition (35). When μ_Z(t) varies between μ_{Z1} and μ_{Z2} the gimbal motion is asymptotically stable. The case $\mu_Z(t) = \mu_{ZC} + \neg \sin \mu t$ oscillating near the stability boundary μ_{Z2} is studied by numerical simulation of the system (4) as shown in figures 14-15. In figure 14(a)-(b), the trajectories of the perturbed motion asymptotically converges to the origin from the initial state (x_1, x_2, x_3)=(0.1,0,0) when μ_Z(t) oscillates between μ_{Z1} and μ_{Z2}. The quasi-periodic trajectory is restricted to an annular-like region of the state space and the corresponding Poincaré map points fill in an elliptically shaped closed curve for μ_{ZC} = 2000, ¬=0.415 at the fixed driving frequency μ = 30 in Figure 14 (c) and (d), respectively. A limit cycle of period-T plotted in phase plane for ¬=1.25 as shown in figure 15(a). From figure 15(b)-(d), the time history, phase portraits and Poincaré maps exhibit the chaotic motion of the system for ¬=1.31.

6. CONCLUSIONS

An analysis is presented of a single-axis rate gyro with torque control in vibratory situation. . For the autonomous case in which μ_Z is steady, both stability and degeneracy conditions of the fixed point were derived by the Routh-Hurwitz criterion in section 3.1. For the nonautonomous case in which $\mu_Z(t)$ and $\dot{\mu}_X(t)$ are time-varying, the differential equation of motion contains explicit functions of time as coefficient. It is more difficult to find the Liapunov function candidate than that of the autonomous system by using the Liapunov direct method. The conditions sufficient for asymptotic stability and instability of motion were obtained in section 3.2. In section 4, the electric time constant is much smaller than the mechanical time constant is assumed. Then modeling this physical system in the singularly perturbed form can be found. The stability of a full singular perturbed system from the reduced and boundary-layer systems was studied by the Liapunov direct method for sufficiently small £. In this paper, the model considered here provides not only conditions sufficient for asymptotic stability for design but also the existence of periodic, quasiperiodic and chaotic motions of the system. Finally, the occurrence and nature of chaotic attractors were studied by evaluating the time history, phase plane and Poincaré maps

五、References

1 S.N. SINGH 1981 *IEEE Transactions on Aerospace and Electronic Systems*, **AES-17**, 208-211. Stability of Gyro in a Vehicle Spinning with Uncertain Angular Vehicle.

2 S.N. SINGH 1983 *IEEE Transactions on Aerospace and Electronic Systems*, **AES-19**, 182-189. Stability of Gyro with Harmonic Nonlinearity in Spinning Vehicle.
3 S.N. SINGH 1984 *IEEE Transactions on Aerospace and Electronic Systems*, **AES-20**, 119-127. Gyro Motion Boundedness Under Uncertain Vehicle Spin and Acceleration.
4 Z. M. GE and C. J. CHEN 1992 *AIAA Journal of Guidance, Control, and Dynamics*, **15**, 1034-1036. Stability of a Rate Gyro.
5 Z. M. GE and H. H. CHEN 1997 *Jpn. J. Appl. Phys*, **36**, 5373-5381. Stability and Chaotic Dynamics of a Rate Gyro with Feedback Control.
6 F. C. Moon 1987 *Chaotic Vibrations*. New York: John Wiley and Sons.
7 J.M.T. THOMPSON and H.B. STEWART 1986 *Nonlinear Dynamics Chaos*. Chichester: Wiley
8 M. LASKSHMANAN and K. MURALI 1996 *Chaos in Nonlinear Oscillators: Controlling and Synchronization*. Singapore: World Scientific.
9 P. HOLMES 1985 *Trans. ASME J. Dyn. Sys. Meas. Control*, **107**, 159-165. Dynamics of a Nonlinear Oscillator with Feedback Control I: Local Analysis.
10 J. GUCKENHEIMER and P. HOLMES 1986 *Nonlinear Oscillations, Dynamical Systems and Bifurcation of Vector Fields*. New York: Springer-Verlag. Chaps. 4-7.
11 G. PEPONIDES, P. V. KOKOTOVIC and J. H. CHOW 1982 *IEEE Transactions Circuits and Systems*, **CAS-29**, 758-767. Singular Perturbations and Time Scales in Nonlinear Models of Power Systems.
12 H. K. KHALIL 1992 *Nonlinear Systems*. New York: Macmillan. Chap. 8.
13 L. MEIROVITCH 1970 *Method of Analytical Dynamics*. New York: McGraw-Hill. Chaps. 6-7, 10.

APPENDIX (I)

The stability analysis that describes a procedure for constructing Liapunov functions for full singularly perturbed system as follows [12]:

Consider the singularly perturbed nonautonomous system

$$\dot{x} = f(t, x, z, \varepsilon)$$
$$\varepsilon \dot{z} = g(t, x, z, \varepsilon)$$

Assume that the following assumptions are satisfied for all

$$(t, x, \varepsilon) \in [0, \infty) \times B_r \times [0, \varepsilon_0]$$

(1) $f(t,0,0,\varepsilon) = 0$ *and* $g(t,0,0,\varepsilon) = 0$.

(2) The equation $0 = g(t, x, z, 0)$ has an isolated root $z = h(t, x)$ such that $h(t, x) = 0$.

(3) The functions f, g and h and their partial derivatives up to order 2 are bounded for $z - h(t, x) \in B_\rho$.

(4) The origin of the reduced system $\dot{x} = f(t, x, h(t, x), 0)$ is exponentially stable.

(5) The origin of the boundary-layer system $\frac{dy}{d\tau} = g(t, x, y + h(t, x), 0)$ is exponentially uniformly stable in (t, x).

Then there exists $\varepsilon^* > 0$ such that, for all ε^*, the origin of (I1) is exponentially stable.

APPENDIX (II)

The values of gyro parameters:

$(A + A_g) = 54\ dyne \cdot cm \cdot s^2$, $Cn_R = 10.8 \times 10^4\ dyne \cdot cm \cdot s$, $C_d = 756$

,

$D_1 = \frac{C_d}{(A+A_g)} = 130\text{-}150\ rad^{-1} \cdot s^{-1}$, $D_2 = \frac{K_T}{(A+A_g)} = 380\text{-}400\ A^{-1} \cdot rad^{-2} \cdot s^{-2}$, $D_3 = \frac{Cn_R}{(A+A_g)} = 2000\ s^{-1}$,

$D_4 = \frac{(A+B_g-C_g)}{(A+A_g)} = 1$, $D_5 = R/L = 25\ sec^{-1}$, $D_6 = K_a/L = 2500\ A\ rad^{-1} \cdot s^{-1}$, $D_7 = K_b/L = 1\ A\ rad^{-1}$

(a)

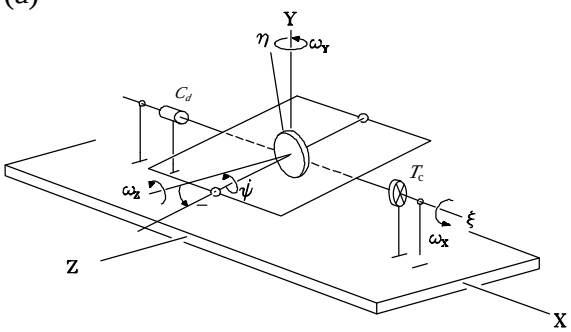

(b)

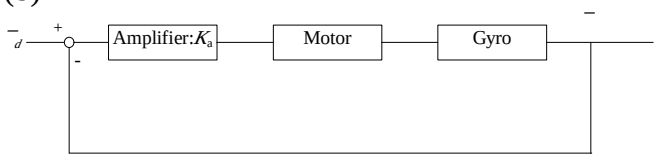

Figure 1. The feedback system (a) The rate gyro, (b) The block diagram.

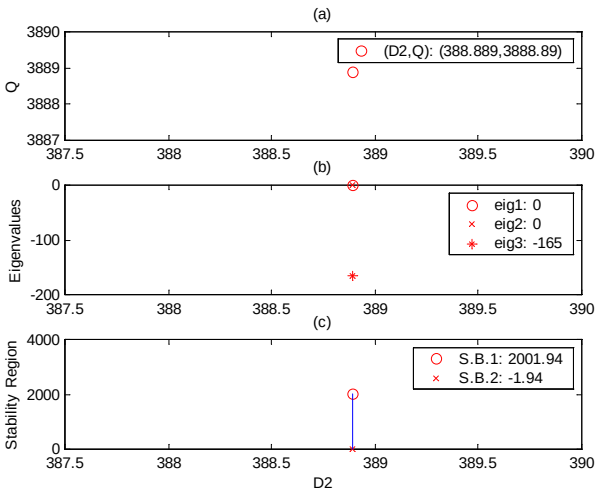

Figure 2. Stability analysis of the autonomous system (5) for the system parameters (D_2, Q) = (388.889,3888.89); (a) the double-zero degeneracy in this system, (b) double-zero eigenvalues with the third eigenvalue $a_3 = -165$, (c) the stability boundary of the uncertain constant angular velocity μ_{ZC}.

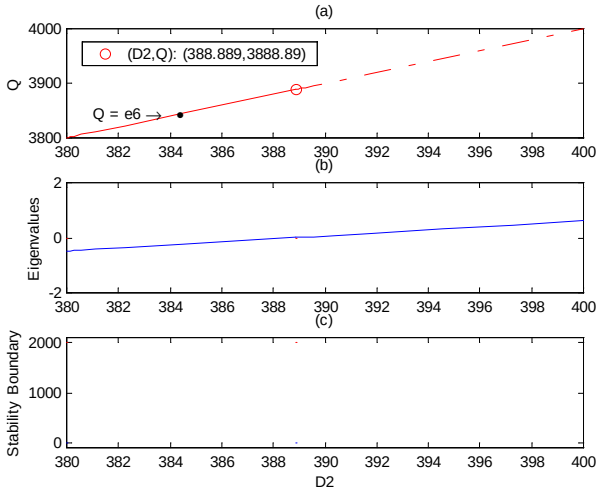

Figure 3. Stability analysis of the autonomous system (5) near the double-zero degenerate point (D_2, Q) = (388.889,3888.89); (a) one zero eigenvalue at $Q=e_6$, (b) two maximum eigenvalues of the system corresponding $Q=e_6$., (c) the stability boundary of the uncertain constant angular velocity μ_{ZC} corresponding $Q=e_6$.

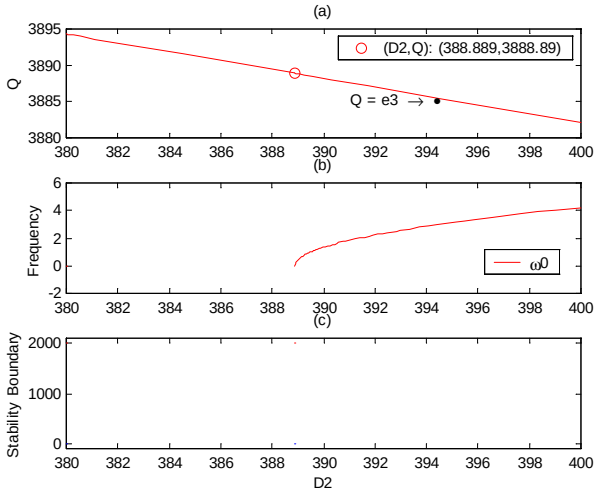

Figure 4. Stability analysis of the autonomous system (5) near the double-zero degenerate point (D_2, Q) = (388.889,3888.89); (a) one eigenvalue with zero real part at $Q=e_3$, (b) a pair of pure imaginary eigenvalues corresponding $Q=e_3$, (c) the stability boundary of the uncertain constant angular velocity μ_{ZC} corresponding $Q=e_3$.

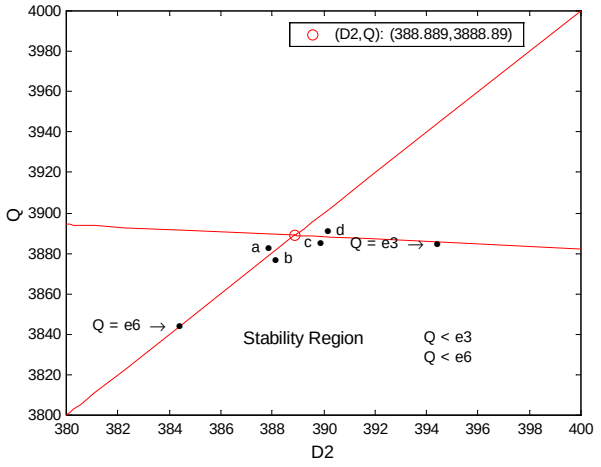

Figure 5. Stability region of the autonomous system (5) near the double-zero degenerate point (D_2, Q) = (388.889,3888.89).

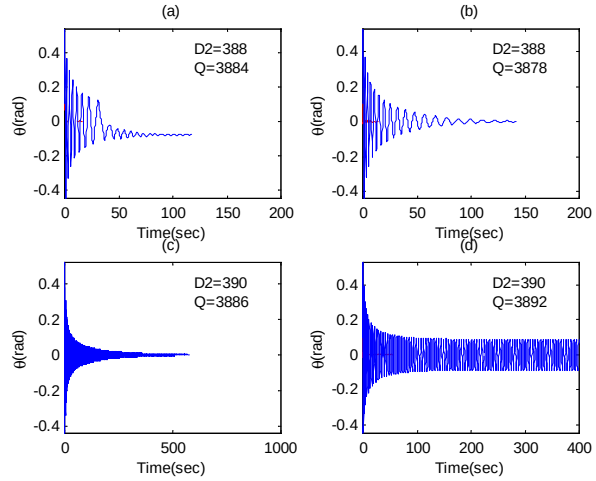

Figure 6. The time histories of the autonomous system (5) near the double-zero degenerate point (D_2, Q) = (388.889,3888.89); (a) 'a' point (D_2, Q) = (388,3884), (b) 'b' point (D_2, Q) = (388,3878), (c) 'c' point (D_2, Q) = (390,3886), (d) 'd' point (D_2, Q) = (390,3892) in figure 5.

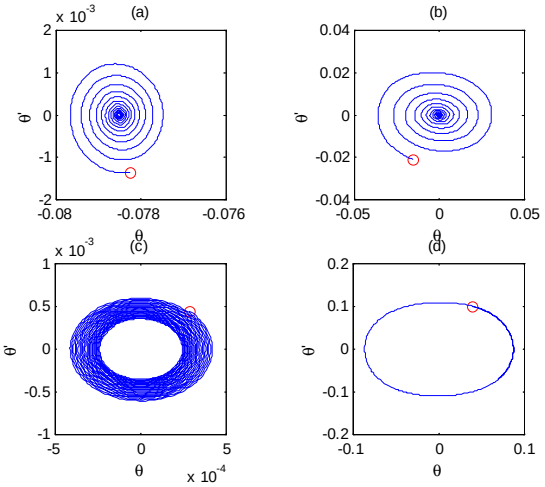

Figure 7. The phase trajectories of the autonomous system (5) near the double-zero degenerate point (D_2, Q) = (388.889,3888.89); (a) 'a' point (D_2, Q) = (388,3884), (b) 'b' point (D_2, Q) = (388,3878), (c) 'c' point (D_2, Q) = (390,3886), (d) 'd' point (D_2, Q) = (390,3892) in figure 5.

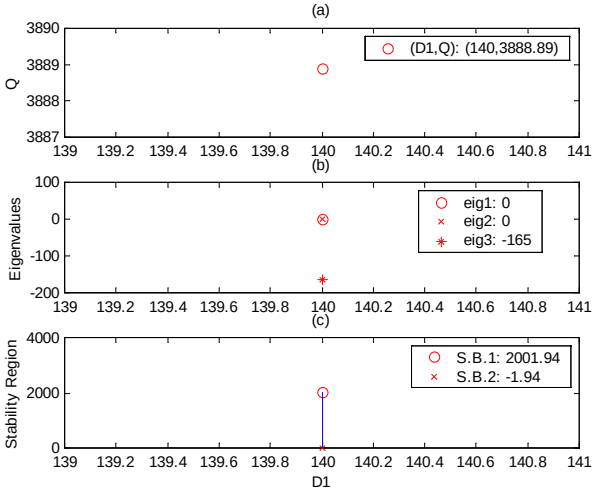

Figure 8. Stability analysis of the autonomous system (5) for the system parameters (D_1, Q) = (140,3888.89); (a) the double-zero degeneracy in this system, (b) double-zero eigenvalues with the third eigenvalue a_3= –165, (c) the stability boundary of the uncertain constant angular velocity μ_{ZC}.

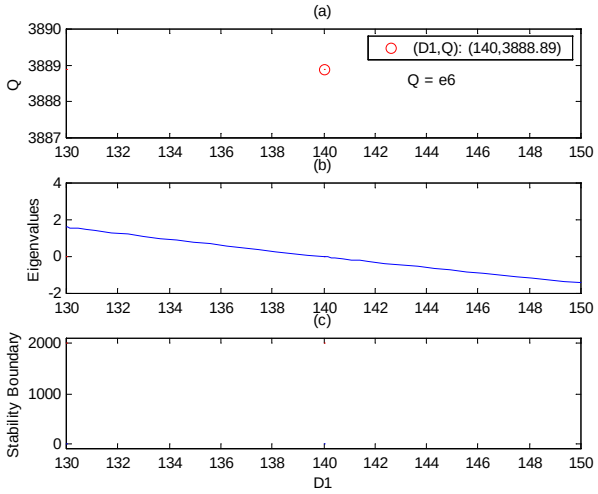

Figure 9. Stability analysis of the autonomous system (5) near the double-zero degenerate point (D_1, Q) = (140,3888.89); (a) one zero eigenvalue at $Q=e_6$, (b) two maximum eigenvalues of the system corresponding $Q=e_6$, (c) the stability boundary of the uncertain constant angular velocity μ_{ZC} corresponding $Q=e_6$.

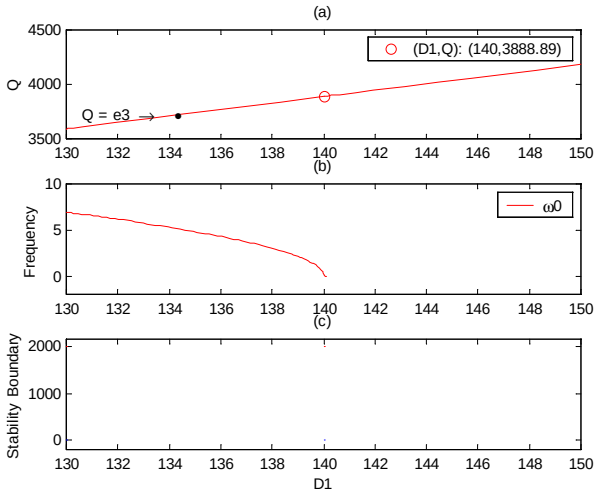

Figure 10. Stability analysis of the autonomous system (5) near the double-zero degenerate point (D_1, Q) = (140,3888.89); (a) one eigenvalue with zero real part at $Q=e_3$, (b) a pair of pure imaginary eigenvalues corresponding $Q=e_3$, (c) the stability boundary of the uncertain constant angular velocity μ_{ZC} corresponding $Q=e_3$.

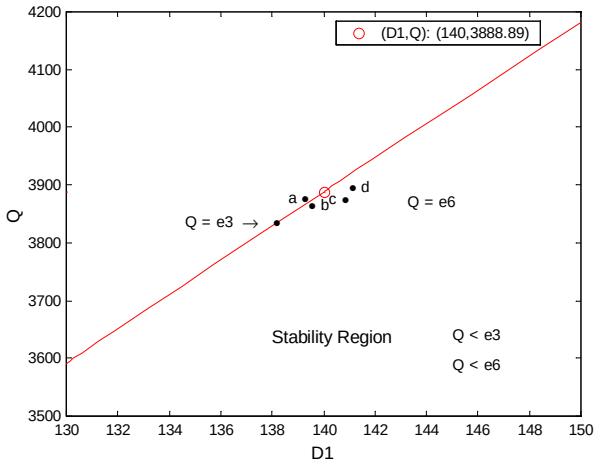

Figure 11. Stability region of the autonomous system (5) near the double-zero degenerate point (D_1, Q) = (140,3888.89).

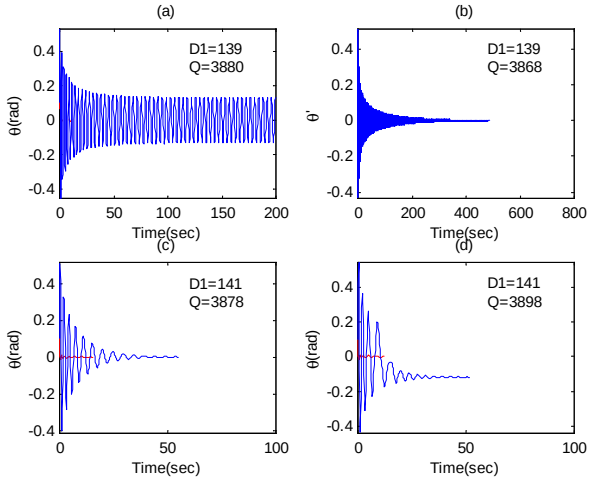

Figure 12. The time histories of the autonomous system (5) near the double-zero degenerate point (D_1, Q) = (140,3888.89); (a) 'a' point (D_1, Q) = (139,3880), (b) 'b' point (D_1, Q) = (139,3868), (c) 'c' point (D_1, Q) = (141,3878), (d) 'd' point (D_1, Q) = (141,3898) in figure 11.

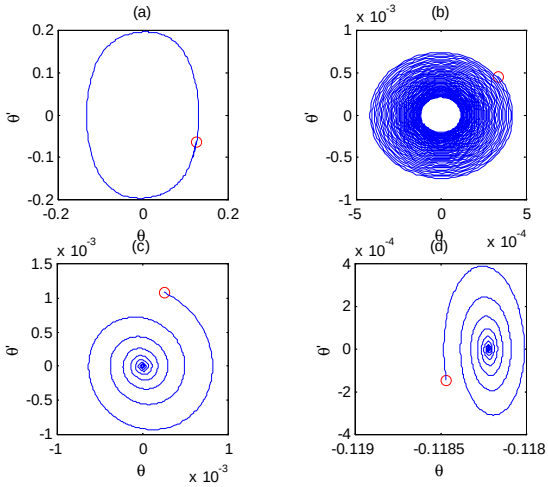

Figure 13. The phase trajectories of the autonomous system (5) near the double-zero degenerate point (D_1, Q) = (140,3888.89); (a) 'a' point (D_1, Q) = (139,3880), (b) 'b' point (D_1, Q) = (139,3868), (c) 'c' point (D_1, Q) = (141,3878), (d) 'd' point (D_1, Q) = (141,3898) in figure 11.

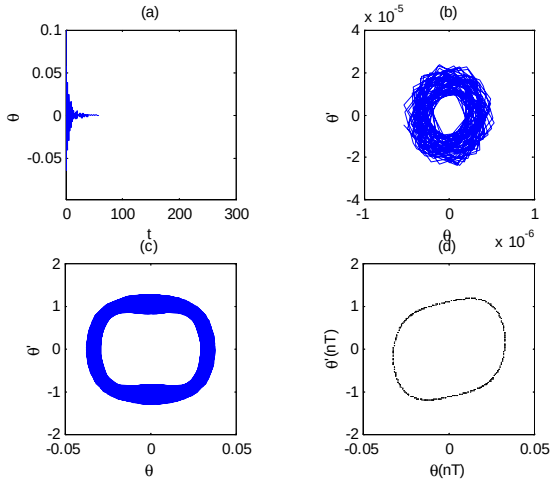

Figure 14. The numerical simulation of the nonautonomous system (4); (a) the time history, (b) the phase trajectory for $\mu_Z(t)$ = 1999+0.415sin(30t); (c) the phase trajectory, (d) Poincaré map for $\mu_Z(t)$ = 2000+0.415sin(30t).

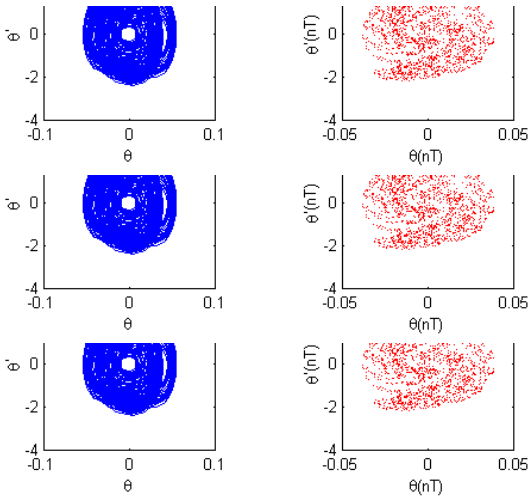

Figure 15. The numerical simulation of the nonautonomous system (4); (a) the phase trajectory for $\mu_Z(t)$ = 2000+1.25*sin*(30*t*); (b) the time history, (c) the phase trajectory, (d) Poincaré map for $\mu_Z(t)$ = 2000+1.31*sin*(30*t*).